15th Triennial World Congress, Barcelona, Spain

PHYSICAL PARAMETER IDENTIFICATION OF A MAGNETIC LEVITATION SYSTEM UNDER A ROBUST NONLINEAR CONTROLLER

Zi-Jiang Yang, Kouichi Miyazaki, Chun-Zhi Jin, and Kiyoshi Wada

* *Department of Electrical and Electronic Systems Engineering, Kyushu University, Hakozaki, Fukuoka 812-8581, Japan*
TEL: (+81)92-642-3904, FAX: (+81)92-642-3939
E-mail: yoh@ees.kyushu-u.ac.jp

Abstract: *In this paper, we propose an efficient procedure of physical parameter identification of a magnetic levitation system, where the levitated steel ball is controlled by a robust nonlinear controller which is designed based on rough nominal parameters. Design techniques of the robust nonlinear controller are described and parameter identification results are included. Finally, it is shown that position tracking performance can be improved by using the identified parameters. Copyright ©2002 IFAC*

Keywords: Magnetic levitation system, closed-loop, physical parameter identification. least-squares method. robust nonlinear control.

1. INTRODUCTION

Due to strong open-loop instablility and inherent nonlinearities, the control problem of a magnetic levitation system is usually quite challenging to the control engineers. Practically, it is often of particular interest to know the exact physical parameters of the system under study, for system simulation, analysis and control performance assessment. In this paper, we first propose a robust nonlinear controller in the presence of parametric uncertainties. This makes it possible to identify the physical parameters accurately in closed-loop, where the robust controller is designed based on rough nominal parameters. Then we propose an efficient procedure of physical parameter identification of a magnetic levitation system.

2. MODEL OF THE MAGNETIC LEVITATION SYSTEM

Consider the magnetic levitation system shown in Fig. 1, whose dynamics can be described in the following equations (Joo and Seo, 1997).

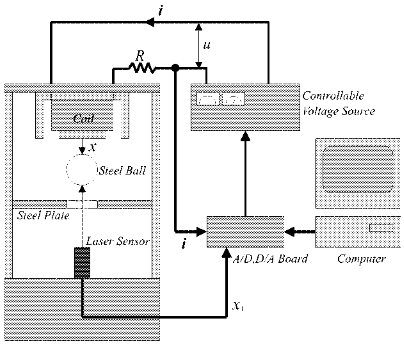

Fig. 1. Diagram of the magnetic levitation system.

$$\begin{bmatrix} \dot{x}_1 \\ \dot{x}_2 \\ \dot{x}_3 \end{bmatrix} = \begin{bmatrix} x_2 \\ \alpha(\boldsymbol{x}) \\ \beta(\boldsymbol{x}) \end{bmatrix} + \begin{bmatrix} 0 \\ 0 \\ \gamma(\boldsymbol{x}) \end{bmatrix} u + \begin{bmatrix} 0 \\ g \\ 0 \end{bmatrix} \quad (1)$$

$$\begin{aligned} \alpha(\boldsymbol{x}) &= -\frac{Qx_3^2}{2M(X_\infty + x_1)^2} \\ \beta(\boldsymbol{x}) &= \frac{x_3\{Qx_2 - R(X_\infty + x_1)^2\}}{Q(X_\infty + x_1) + L_\infty(X_\infty + x_1)^2} \\ \gamma(\boldsymbol{x}) &= \frac{X_\infty + x_1}{Q + L_\infty(X_\infty + x_1)} \end{aligned} \quad (2)$$

where $\boldsymbol{x} = [x_1, x_2, x_3]^T = [x, \dot{x}, i]^T$ is state variable vector. And, x: air gap (vertical position) of the steel ball; i: coil current; g: gravity acceleration; M: mass of the steel ball; R: electrical resistance; u: voltage control input; L_∞, Q and X_∞: positive constants determined by the characteristics of the coil, magnetic core and steel ball.

Denote the nominal physical parameters as g_0, M_0, R_0, $L_{\infty 0}$, Q_0 and $X_{\infty 0}$, we have the nominal nonlinear functions and the modelling errors respectively as the following.

$$\begin{aligned}\alpha_0(\boldsymbol{x}) &= -\frac{Q_0 x_3^2}{2M_0(X_{\infty 0}+x_1)^2}\\ \beta_0(\boldsymbol{x}) &= \frac{x_3\{Q_0 x_2 - R_0(X_{\infty 0}+x_1)^2\}}{Q_0(X_{\infty 0}+x_1)+L_{\infty 0}(X_{\infty 0}+x_1)^2}\\ \gamma_0(\boldsymbol{x}) &= \frac{X_{\infty 0}+x_1}{Q_0+L_{\infty 0}(X_{\infty 0}+x_1)}\end{aligned} \quad (3)$$

$$\begin{aligned}\Delta_\alpha(\boldsymbol{x}) &= \alpha(\boldsymbol{x}) - \alpha_0(\boldsymbol{x})\\ \Delta_\beta(\boldsymbol{x}) &= \beta(\boldsymbol{x}) - \beta_0(\boldsymbol{x})\\ \Delta_\gamma(\boldsymbol{x}) &= \gamma(\boldsymbol{x}) - \gamma_0(\boldsymbol{x})\end{aligned} \quad (4)$$

3. COORDINATE TRANSFORMATION

To convert the original nonlinear system into a system that is "simpler" in the sense that controller synthesis is more straightforward, we adopt the following nonlinear coordinate transformation (Isidori, 1995).

$$\boldsymbol{\xi} = [\xi_1,\ \xi_2,\ \xi_3]^T = [x_1,\ x_2,\ \alpha_0(\boldsymbol{x})]^T \quad (5)$$

Remark 1: According to Fig. 1, the diffeomorphim $\boldsymbol{\xi} = \boldsymbol{T}(\boldsymbol{x})$ is only locally defined in a compact feasible region $\Omega_x = \{\boldsymbol{x} \big| 0 \le x_1 \le x_{1M},\ x_3 > 0\} \subset R^3$, no matter what the control strategy is.

Hence the nonlinear state space model (1) is transformed into

$$\begin{aligned}\dot{\xi}_1 &= \xi_2\\ \dot{\xi}_2 &= g_0 + \Delta_g + \xi_3\left(1+\frac{\Delta_\alpha(\boldsymbol{x})}{\alpha_0(\boldsymbol{x})}\right)\\ \dot{\xi}_3 &= F_1(\boldsymbol{x}) + F_0(\boldsymbol{x}) + \Delta_F(\boldsymbol{x}) + u\,(G_0(\boldsymbol{x}) + \Delta_G(\boldsymbol{x}))\end{aligned} \quad (6)$$

where

$$F_1(\boldsymbol{x}) = \frac{Q_0 x_3^2}{M_0(X_{\infty 0}+x_1)^3} x_2 \quad (7)$$

$$F_0(\boldsymbol{x}) = -\frac{Q_0 x_3^2\left\{Q_0 x_2 - R_0(X_{\infty 0}+x_1)^2\right\}}{(X_{\infty 0}+x_1)^3\{Q_0+L_{\infty 0}(X_{\infty 0}+x_1)\}} \quad (8)$$

$$G_0(\boldsymbol{x}) = -\frac{Q_0 x_3}{M_0(X_{\infty 0}+x_1)\{Q_0+L_{\infty 0}(X_{\infty 0}+x_1)\}} \quad (9)$$

$$\Delta_F(\boldsymbol{x}) = -\frac{Q_0 x_3}{M_0(X_{\infty 0}+x_1)^2}\Delta_\beta(\boldsymbol{x}) \quad (10)$$

$$\Delta_G(\boldsymbol{x}) = -\frac{Q_0 x_3}{M_0(X_{\infty 0}+x_1)^2}\Delta_\gamma(\boldsymbol{x}) \quad (11)$$

4. DESIGN OF THE CONTROLLER

It is assumed here that the reference position y_r of the steel ball and its first, second and third derivatives, i.e., $\dot{y}_r$, $\ddot{y}_r$ and $y_r^{(3)}$ are continuous, uniformly bounded, and available.

Step 1:

Define the error signals of ξ_1 and ξ_2 as

$$z_1 = \xi_1 - y_r, \quad z_2 = \xi_2 - \alpha_1 \quad (12)$$

where α_1 is a virtual input to stabilize z_1.

Then we have subsystem $\mathcal{S}1$ as the following.

$$\dot{z}_1 = \alpha_1 + z_2 - \dot{y}_r \quad (13)$$

The virtual input α_1 is designed based on the common PI control technique.

$$\alpha_1 = -c_{1p} z_1 - c_{1i}\int_0^t z_1\ dt + \dot{y}_r \quad (14)$$

where $c_{1p} > 0,\ c_{1i} > 0$.

Denote the Laplace operator as s. Then subsystem $\mathcal{S}1$ controlled by α_1 can be expressed as

$$z_1 = \frac{s z_2}{s^2 + c_{1p}s + c_{1i}} \quad (15)$$

Therefore, if the velocity error z_2 is stabilized to a neighbourhood of the origin, $|z_1|$ can be made sufficiently small, and the offset of z_1 can be removed by the integrator.

Equation (15) can be put into the following state-space model.

$$\dot{\boldsymbol{z}}_{1a} = \boldsymbol{A}\ \boldsymbol{z}_{1a} + \boldsymbol{B}\ z_2 \quad (16)$$

where $\boldsymbol{z}_{1a} = [\int_0^t z_1\ dt,\ z_1]^T$ and

$$\boldsymbol{A} = \begin{bmatrix} 0 & 1 \\ -c_{1i} & -c_{1p} \end{bmatrix}, \quad \boldsymbol{B} = [0 \quad 1]^T \quad (17)$$

As a preparation for the input-to-state stability (ISS) [1] analysis of the overall error system discussed later, we have here the ISS of subsystem $\mathcal{S}1$ with respect to z_2 by lemma 1.

Lemma 1. If z_2 is continuous and uniformly bounded, then $\mathcal{S}1$ is ISS, i.e., for $^\exists\lambda_0 > 0, {}^\exists\alpha_0 > 0$ and $^\exists M > 0$,

$$|\boldsymbol{z}_{1a}(t)| \le \lambda_0 e^{-\alpha_0 t}|\boldsymbol{z}_{1a}(0)| + M\left[\sup_{0\le\tau\le t}|z_2(\tau)|\right]$$

Step 2:

Define

$$z_3 = \xi_3 - \alpha_2 \quad (18)$$

where α_2 is a virtual input to stabilize z_2.

[1] In this paper, both Input-to-State Stability and Input-to-State Stable will be denoted as ISS for convenience.

Then we have subsystem $\mathcal{S}2$ as

$$\dot{z}_2 = -\dot{\alpha}_1 + g_0 + \Delta_g + \alpha_2 + \alpha_2 \frac{\Delta_\alpha(\boldsymbol{x})}{\alpha_0(\boldsymbol{x})} + z_3 \frac{\alpha(\boldsymbol{x})}{\alpha_0(\boldsymbol{x})} \quad (19)$$

Motivated by the works of Krstic *et al.* (1995), we design the virtual input α_2 as the following to stabilize subsystem $\mathcal{S}2$.

$$\begin{aligned} \alpha_2 &= \alpha_{20} - \alpha_{21} - \alpha_{22} \\ \alpha_{20} &= -c_2 z_2 + \dot{\alpha}_1 - g_0 \\ \alpha_{21} &= \kappa_{21} g_0 z_2 \\ \alpha_{22} &= \kappa_{22} \sqrt{\alpha_{20}^2 + \nu} z_2 \end{aligned} \quad (20)$$

where $c_2 > 0,\ \kappa_{21} > 0,\ \kappa_{22} > 0,\ \nu = 0.01$. α_{20} is a feedback linearization controller of the nominal system model, while α_{21} is a linear damping term to counteract Δ_g, and α_{22} is a nonlinear damping term to counteract Δ_α.

Applying the virtual input α_2, we have

$$\begin{aligned} \dot{z}_2 = &-c_2 z_2 - \left(\kappa_{21} g_0 z_2 + \kappa_{22}\sqrt{\alpha_{20}^2 + \nu} z_2\right) \frac{\alpha(\boldsymbol{x})}{\alpha_0(\boldsymbol{x})} \\ &+ \Delta_g + \frac{\Delta_\alpha(\boldsymbol{x})}{\alpha_0(\boldsymbol{x})}\alpha_{20} + \frac{\alpha(\boldsymbol{x})}{\alpha_0(\boldsymbol{x})} z_3 \end{aligned} \quad (21)$$

Based on equations (20) and (21), we can show the following result:

Lemma 2. If z_3 is continuous and uniformly bounded, then $\mathcal{S}2$ is ISS such that

$$|z_2(t)| \le |z_2(0)| e^{-c_2 t/2} + \sup_{0 \le \tau \le t} [\mu_{21}(\tau) + \mu_{22}(\tau) z_3]$$

with respect to the following continuous and uniformly bounded functions.

$$\mu_{21}(t) = \frac{|\Delta_g| + \left|\frac{\Delta_\alpha(\boldsymbol{x})}{\alpha_0(\boldsymbol{x})}\alpha_{20}\right|}{\frac{c_2}{2} + \frac{\alpha(\boldsymbol{x})}{\alpha_0(\boldsymbol{x})}\left(\kappa_{21} g_0 + \kappa_{22}\sqrt{\alpha_{20}^2 + \nu}\right)}$$

$$\mu_{22}(t) = \frac{\frac{\alpha(\boldsymbol{x})}{\alpha_0(\boldsymbol{x})}}{\frac{c_2}{2} + \frac{\alpha(\boldsymbol{x})}{\alpha_0(\boldsymbol{x})}\left(\kappa_{21} g_0 + \kappa_{22}\sqrt{\alpha_{20}^2 + \nu}\right)}$$

Step 3:

Through straightforward but tedious calculations based on some previous equations, we have

$$\dot{\alpha}_2 = F_2 - F_3(\alpha_0 + g_0) - F_3(\Delta_\alpha + \Delta_g) \quad (22)$$

$$\begin{aligned} F_2 = &\\ &\left\{1 - \kappa_{22}(\alpha_{20}^2 + \nu)^{-0.5}\alpha_{20} z_2\right\}\left\{c_{1p}\ddot{y}_r - c_{1i}\dot{z}_1 + y_r^{(3)}\right\} \\ &+ c_2\left\{1 - \kappa_{22}(\alpha_{20}^2 + \nu)^{-0.5}\alpha_{20} z_2\right\}\dot{\alpha}_1 \\ &+ \left\{\kappa_{21} g_0 + \kappa_{22}(\alpha_{20}^2 + \nu)^{0.5}\right\}\dot{\alpha}_1 \end{aligned} \quad (23)$$

$$\begin{aligned} F_3 = &c_2 + c_{1p} + \kappa_{21} g_0 + \kappa_{22}(\alpha_{20}^2 + \nu)^{0.5} \\ &-(c_2 + c_{1p})\kappa_{22}(\alpha_{20}^2 + \nu)^{-0.5}\alpha_{20} z_2 \end{aligned} \quad (24)$$

Then we have subsystem $\mathcal{S}3$ as

$$\begin{aligned} \dot{z}_3 &= \dot{\xi}_3 - \dot{\alpha}_2 \\ &= \Psi_0 + \Delta_\Psi(\boldsymbol{x}) + G_0(\boldsymbol{x})u + \Delta_G(\boldsymbol{x})u \end{aligned} \quad (25)$$

where

$$\begin{aligned} \Psi_0 &= F_0 + F_1 - F_2 + F_3(\alpha_0 + g_0) \\ \Delta_\Psi(\boldsymbol{x}) &= \Delta_F(\boldsymbol{x}) + F_3(\Delta_\alpha(\boldsymbol{x}) + \Delta_g) \end{aligned} \quad (26)$$

Similar to the design technique in step 2, the control input is designed as

$$\begin{aligned} u &= \frac{\alpha_{30} - \alpha_{31} - \alpha_{32} - \alpha_{33}}{G_0(\boldsymbol{x})} \\ \alpha_{30} &= -c_3 z_3 - \Psi_0 \\ \alpha_{31} &= \kappa_{31}\left(1 - 0.5e^{-\lambda_1|z_3|}\right) F_{0d} z_3 \\ \alpha_{32} &= \kappa_{32}\left(1 - 0.5e^{-\lambda_2|z_3|}\right) |F_3|(|\alpha_0| + g_0) z_3 \\ \alpha_{33} &= \kappa_{33}\left(1 - 0.5e^{-\lambda_3|z_3|}\right) |\alpha_{30}| z_3 \end{aligned} \quad (27)$$

where $c_3 > 0,\ \kappa_{31} > 0,\ \kappa_{32} > 0,\ \kappa_{33} > 0$, and

$$F_0 = \frac{Q_0 x_3^2\{Q_0|x_2| + R_0(X_{\infty 0} + x_1)^2\}}{(X_{\infty 0} + x_1)^3\{Q_0 + L_{\infty 0}(X_{\infty 0} + x_1)\}} \quad (28)$$

Here, α_{30} is a feedback linearization controller, and α_{31}, α_{32} and α_{33} are nonlinear damping terms employed to counteract the modelling errors Δ_F, $F_3(\Delta_\alpha + \Delta_G)$ and Δ_G respectively. Also, notice that $(1 - 0.5e^{-\lambda_i|z_3|}),\ i = 1, 2, 3$ are introduced to reduce control efforts due to the nonlinear damping terms, when $|z_3|$ is relatively small.

When the designed u is applied to subsystem $\mathcal{S}3$, its dynamics becomes

$$\begin{aligned} \dot{z}_3 = &-c_3 z_3 + \Delta_F(\boldsymbol{x}) + F_3(\Delta_\alpha(\boldsymbol{x}) + \Delta_g) \\ &+ \frac{\Delta_G(\boldsymbol{x})}{G_0(\boldsymbol{x})}\alpha_{30} - G(\boldsymbol{x})\frac{\alpha_{31} + \alpha_{32} + \alpha_{33}}{G_0(\boldsymbol{x})} \end{aligned} \quad (29)$$

Similar to those in step 2, we have the ISS of subsystem $\mathcal{S}3$ as shown in the following lemma.

Lemma 3. Assume that $\boldsymbol{x}$ stays in the feasible region $\Omega_x = \{\boldsymbol{x} | 0 \le x_1 \le x_{1M},\ x_3 > 0\}$. If the control input u is applied to subsystem $\mathcal{S}3$, then $\mathcal{S}3$ is ISS:

$$|z_3(t)| \le |z_3(0)| e^{-c_3 t/2} + \sup_{0 \le \tau \le t} \mu_3(\tau)$$

with respect to the following continuous and uniformly bounded function.

$$\mu_3(t) = \frac{|\Delta_F(\boldsymbol{x})| + |F_3(\Delta_\alpha(\boldsymbol{x}) + \Delta_g)| + \left|\frac{\Delta_G(\boldsymbol{x})\alpha_{30}}{G_0(\boldsymbol{x})}\right|}{\frac{c_3}{2} + \frac{G(\boldsymbol{x})(\kappa_{31}F_{0d} + \kappa_{32}|F_3|(|\alpha_0| + g_0) + \kappa_{33}|\alpha_{30}|)}{2G_0(\boldsymbol{x})}}$$

5. PARAMETER DESIGN AND TRAJECTORY INITIALIZATION

It is recommendable to choose modest $\kappa_{21},\ \kappa_{22},\ \kappa_{31},\ \kappa_{32},\ \kappa_{33}$ to avoid noisy or large control efforts. In contrast, $c_{1p},\ c_{1i},\ c_2,\ c_3$ can be chosen relatively large, without causing large amplitude of the control input. To further improve the position tracking error $|z_1|$ with moderate control efforts, more accurate nominal physical parameters are helpful, as shown later in Figs. 6∼7.

Lemmas 1 ∼ 3 imply that the initial conditions $z_1(0)$, $z_2(0)$, $z_3(0)$ can influence the transient performance significantly. Suppose the steel ball is initially at rest with $x_1(0) = x_{1M}$ and $x_2(0) = 0$, then if we choose the initial conditions of the reference trajectory such that $y_r(0) = x_1(0)$ and $\dot{y}_r(0) = \ddot{y}_r(0) = 0$, we have $z_1(0) = z_2(0) = 0$. Also from equation (18) we have

$$z_3(0) = g_0 - \frac{Q_0 x_3^2(0)}{2M_0\{X_{\infty 0} + x_1(0)\}^2} \tag{30}$$

Thus $z_3(0)$ can be made relatively small, if we set the initial coil current signal $x_3(0)$ to an appropriate value.

6. STABILITY OF THE OVERALL ERROR SYSTEM

Combining the results of lemmas 1∼3, we have the overall error system as

$$\begin{aligned} |\boldsymbol{z}_{1a}(t)| &\le \lambda_0 e^{-\alpha_0 t}|\boldsymbol{z}_{1a}(0)| + M\left[\sup_{0\le\tau\le t}|z_2(\tau)|\right] \\ |z_2(t)| &\le |z_2(0)|e^{-c_2 t/2} + \sup_{0\le\tau\le t}[\mu_{21}(\tau) + \mu_{22}(\tau)z_3] \\ |z_3(t)| &\le |z_3(0)|e^{-c_3 t/2} + \sup_{0\le\tau\le t}\mu_3(\tau) \end{aligned} \tag{31}$$

Since the overall error system is a cascade of the three ISS subsystems characterized by lemmas 1 ∼ 3 respectively, we can conclude based on lemma C.4 in Krstic *et al.* (1995) that the overall error system is also ISS. Define

$$\boldsymbol{z}(t) = [\boldsymbol{z}_{1a}^T, z_2(t), z_3(t)]^T \tag{32}$$

Then along the same line of the proof of lemma C.4 in Krstic *et al.* (1995), we have the following results.

$$\begin{aligned} |\boldsymbol{z}(t)| \le{} & \beta_3|\boldsymbol{z}(0)|e^{-\rho_2 t} + \sup_{0\le\tau\le t}\mu_3(\tau) \\ & +(\beta_1+1)(\lambda_0 M + M + 1)\left[\sup_{0\le\tau\le t}[\mu_{21}(\tau) + \beta_2\mu_3(\tau)]\right] \end{aligned} \tag{33}$$

where

$$\begin{aligned} \beta_1 &= \max\left(\lambda_0^2, 3M\lambda_0, 3M, 3)\right) \\ \beta_2 &= ||\mu_{22}||_\infty \\ \beta_3 &= \beta_{30}\max\left(\beta_1^2, 3\beta_2(\lambda_0 M + M + 1)\beta_1,\right. \\ &\qquad 3\beta_2(\lambda_0 M + M + 1), 3) \\ \beta_{30} &= \frac{|z_{1i}(0)| + |z_1(0)| + |z_2(0)| + |z_3(0)|}{|\boldsymbol{z}(0)|} \\ \rho_2 &= \min(\alpha_0/4, c_2/8, c_3/4) \end{aligned} \tag{34}$$

However, as mentioned in remark 1, the results obtained here are valid only in $\Omega_x = \{\boldsymbol{x}|0 \le x_1 \le x_{1M},\ x_3 > 0\} \subset R^3$ no matter what the control strategy is. To ensure the controller feasible, we should verify if there is a compact set $\mathcal{D}_x$ such that $\boldsymbol{x} \in \mathcal{D}_x \subset \Omega_x$.

If the smooth reference trajectory is appropriately chosen such that $y_r, \dot{y}_r, \ddot{y}_r, y_r^{(3)} \in \mathcal{D}_{y_r}$ where

$$\begin{aligned} \mathcal{D}_{y_r} = \Big\{ & y_r, \dot{y}_r, \ddot{y}_r, y_r^{(3)} \Big| \ \delta \le y_r \le x_{1M} - \delta, |\dot{y}_r| \le \overline{y}_r, \\ & |\ddot{y}_r| \le \overline{\overline{y}}_r, |y_r^{(3)}| \le \overline{y}_r^{(3)},\ ^\exists\delta, {}^\exists\overline{y}_r, {}^\exists\overline{\overline{y}}_r, \overline{y}_r^{(3)} > 0 \Big\} \end{aligned} \tag{35}$$

then we can make the error signal $\boldsymbol{z}$ stay in a compact set, i.e., $\boldsymbol{z} \in \Omega_z = \{\boldsymbol{z}|\ |\boldsymbol{z}(t)| \le \overline{\boldsymbol{z}},\ ^\exists\overline{\boldsymbol{z}} > 0\} \subset R^4$, where $\overline{\boldsymbol{S}}$ can be made sufficiently small by an appropriate set of reference trajectory, initial states and design parameters, according to inequality (33).

As long as $\boldsymbol{z} \in \Omega_z$, i.e., the steel ball is levitated and tracks a smooth reference trajectory with acceptable accuracy, we can conclude that the electromagnet is exerting an attractive force to counteract the gravity, i.e., $x_3 > 0$ is ensured in generic cases. Therefore we can conclude that there exists a compact set $\mathcal{D}_x$ such that $\boldsymbol{x} \in \mathcal{D}_x \subset \Omega_x$. Finally, based on the above discussions and lemmas 1∼3, we have the following results.

Theorem 1. If the proposed robust nonlinear controller is applied to the magnetic levitation system under study and if the reference trajectory and the initial states are chosen appropriately, the following results hold.

(1) There exists a compact set $\mathcal{D}_x$ such that $\boldsymbol{x} \in \mathcal{D}_x \subset \Omega_x = \{\boldsymbol{x}|0 \le x_1 \le x_{1M},\ x_3 > 0\} \subset R^3$.
(2) The overall error system is ISS such that

$$\begin{aligned} |\boldsymbol{z}(t)| \le{} & \beta_3|\boldsymbol{z}(0)|e^{-\rho_2 t} + \sup_{0\le\tau\le t}\mu_3(\tau) \\ & +(\beta_1+1)(\lambda_0 M + M + 1)\left[\sup_{0\le\tau\le t}[\mu_{21}(\tau) + \beta_2\mu_3(\tau)]\right] \end{aligned}$$

(3) The steady offset of z_1 approaches zero.

3. PHYSICAL PARAMETER IDENTIFICATION

Owing to the proposed robust nonlinear controller, it becomes possible to identify the physical parameters accurately in closed-loop, where the robust controller is designed based on rough nominal parameters. In this section, we propose an efficient procedure of physical parameter identification of a magnetic levitation system.

The nominal parameters provided by the system manual (Japan EM, 1996) are shown in Table 1. It is not easy to verify if they are correct except the mass of the steel ball and the gravity acceleration. To control the steel ball, the robust controller is

Table 1. Physical parameters in the system manual

M	0.54	[kg]
g	9.8	[m/s^2]
X_∞	0.00643	[m]
Q	0.00086173	[Hm]
L_∞	0.7886	[H]
R	11.6	[Ω]

designed based on the following nominal parameters which are rougher than those in Table 1.

$$\begin{aligned} M_0 &= 0.54[\text{kg}],\ g_0 = 9.8[\text{m/s}^2] \\ X_{\infty 0} &= 0.0050[\text{m}],\ Q_0 = 0.0010[\text{Hm}] \\ L_{\infty 0} &= 0.50[\text{H}],\ R_0 = 10.0[\Omega] \end{aligned} \tag{36}$$

Since the unknown parameters appear nonlinearly in equation (1), we propose here a two-stage identificaion procedure based on closed-loop data by virtue of the robust nonlinear controller, such that the linear LS method is applicable. At the first stage, Q and X_∞ of the mechanical motion equation are identified by regulating the steel ball constantly to various desired positions. Then at the second stage, R and L_∞ of the electrical dynamic equation are identified by making the steel ball track a sinusoidal trajectory such that persistently exiciting data for identification are generated. The concrete identification procedure is described as follows.

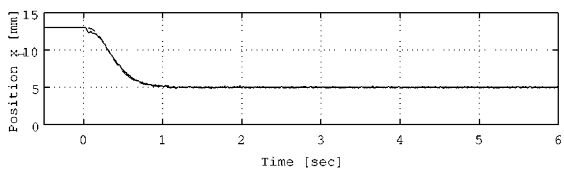

Fig. 2. Position x_1 that is regulated to a constant position.

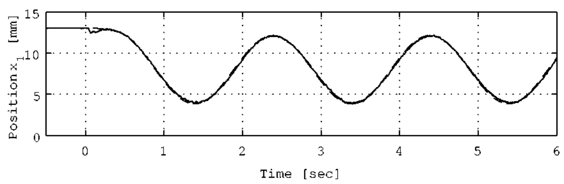

Fig. 3. Position x_1 that tracks a sinusoidal signal.

7.1 *Identification of Q and X_∞*

According to equation (1), we have

$$\dot{x}_2 = g - \frac{Q x_3^2}{2M(X_\infty + x_1)^2} \tag{37}$$

If the steel ball is regulated to a desired constant position, then we have $x_2 \approx 0$ at the steady state and hence

$$\begin{aligned} x_1 &= \boldsymbol{\psi}^T \boldsymbol{\theta} \\ \boldsymbol{\psi}^T &= \left[\sqrt{x_3^2/(2gM)},\ -1\right] \\ \boldsymbol{\theta} &= \left[\sqrt{Q},\ X_\infty\right]^T \end{aligned} \tag{38}$$

Let the steel ball be regulated to various positions such as $12.5, 12.0, 11.5, 11.0, \cdots, 3.5, 3.0$[mm], and measure x_1 and x_3 at the steady-state for each position, then we can identify Q and X_∞ by the linear LS method, if g and M are known. An example of position regulation is shown in Fig. 2.

Remark 3: There is an extensive literature on closed-loop identification for linear transfer function models, see Forssel and Ljung (1999) and the references therein. This case study however, differs from the standard approaches in stochastic framework, such as prediction error method etc. Notice equation (38) describes the static relation of the signals at steady states. At each steady state, the measured x_1 and x_3 are obtained as their averaged measurements over a certain period of time such that the zero-mean noise effects are removed.

7.2 *Identification of R and L_∞*

From equation (1), we have

$$\begin{aligned} \dot{x}_3 = & \frac{\{Q x_2 - R(X_\infty + x_1)^2\} x_3}{Q(X_\infty + x_1) + L_\infty (X_\infty + x_1)^2} \\ & + \frac{(X_\infty + x_1) u}{Q + L_\infty (X_\infty + x_1)} \end{aligned} \tag{39}$$

Replacing the differential operations by the backward finite difference approximation and rearranging equation (39), we have

$$\eta_2(t) = \boldsymbol{\eta}_1^T(t) \boldsymbol{\theta} \tag{40}$$

where

$$\begin{aligned} \boldsymbol{\theta} &= [L_\infty,\ R]^T \\ \boldsymbol{\eta}_1^T(t) &= \left[(X_\infty + x_1)\frac{x_3(t) - x_3(t-T)}{T},\ (X_\infty + x_1) x_3\right] \\ \eta_2(t) &= -Q\frac{x_3(t) - x_3(t-T)}{T} \\ & + \frac{Q x_3 \dfrac{x_1(t) - x_1(t-T)}{T} + (X_\infty + x_1)^2 u}{X_\infty + x_1} \end{aligned} \tag{41}$$

Furthermore, equation (40) can be rewritten as

$$\tilde{\eta}_2(t) = \tilde{\boldsymbol{\eta}}_1^T(t) \boldsymbol{\theta} \tag{42}$$

where

$$\tilde{\boldsymbol{\eta}}_1^T(t) = \frac{\boldsymbol{\eta}_1^T(t)}{(\lambda s + 1)^2},\quad \tilde{\eta}_2(t) = \frac{\eta_2(t)}{(\lambda s + 1)^2} \tag{43}$$

and $1/(\lambda s + 1)^2$ is a lowpass filter employed to reduce the noise effects. In this study, it is chosen such that $\lambda = 0.1$. The lowpass filter is discretized by the bilinear transformation, with sampling interval $T = 0.0005$[sec].

Remark 4: Although the LS method is usually biased in the presence of significant noise, owing to the noise reducing effects by the low-pass filters, in this study, the LS estimate is still satisfactory and reliable, see Fig. 5 which indicates the simulation error of equation (39) with identified physical parameters.

Table 2. Identified parameters

X_∞	0.008114	[m]
Q	0.001624	[Hm]
L_∞	0.7987	[H]
R	11.88	[Ω]

In order to make the regressor $\eta_1^T(t)$ persistently exciting such that L_∞ is identifiable, let the steel ball track a sinusoidal signal as shown in Fig. 3 and measure x_1, x_3 and u with sampling period $T = 0.0005$[sec]. Then R and L_∞ can be identified by the LS method based on equation (41), if Q and X_∞ are already identified as described previously. It should be noticed here that we have verified that the estimates are not sensitive to the period of the sinusoidal signal.

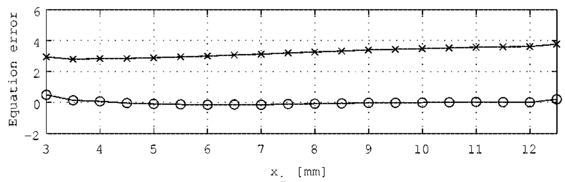

Fig. 4. A comparison of equation errors of equation (3).

7.3 *Identification results*

By using the proposed identification procedure, we have the identified parameters as shown in Table 2. It can be verified that the estimates of R and L_∞ are similar to those in Table 1, while the estimates of Q and X_∞ differ significantly from those in Table 1. To verify the reliability of our results, we show in Fig. 4 the equation errors of equation (37) at various steady positions respectively, where the circles indicate the equation errors by the identified parameters, while the x-marks indicate those by the parameters shown in Table 1. It can be seen that the identified Q and X_∞ yield much smaller equation errors. Also, to evaluate the identified R and L_∞, we show in Fig. 5 the simulation error of $\widehat{x}_3$ obtained by peforming numerical integration on equation (39) where the identified R and L_∞, and those in Table 1 are used respectively (for Q and X_∞, only the identified values are used since they are much more reliable). It can be seen that although both are acceptable, our estimates yield smaller error.

Finally, the position tracking performances for a fast changing reference trajectory by using the physical parameters taken from Table 1 and Table 2 respectively are shown in Figs. 6∼7. It can be verified that the identified physical parameters are helpful to improve the control performance.

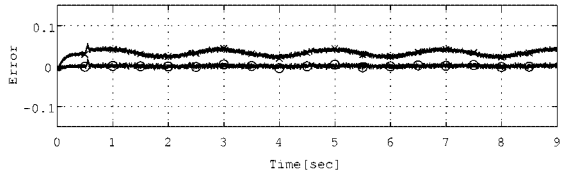

Fig. 5. A comparison of simulation error $\widehat{x}_3 - x_3$.

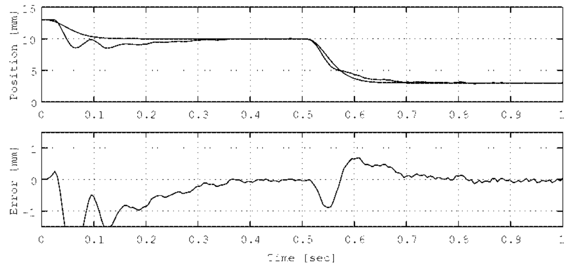

Fig. 6. Performance of position control by the parameters in Table 1.

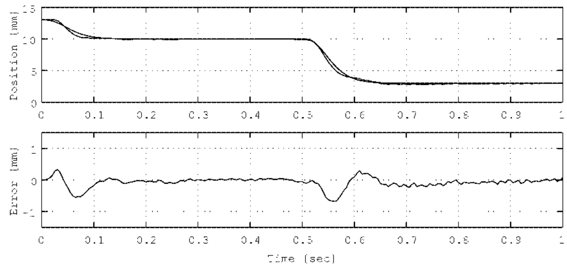

Fig. 7. Performance of position control by the parameters in Table 2.

4. CONCLUSIONS

In this paper, we proposed a robust nonlinear controller via backstepping design approach, for position tracking problem of a voltage controlled magnetic levitation system in the presence of uncertainties of the physical parameters. Then we proposed an efficient procedure of physical parameter identification of a magnetic levitation system in closed-loop, where the levitated steel ball is controlled by the proposed robust nonlinear controller which is designed based on rough nominal parameters. We believe that the identification results are helpful for simulation, analysis and control performance assessment of the system under study.

REFERENCES

Forssell, U., & L. Ljung (1999). Closed-loop identification – revisited, *Automatica, 35*(7), 1215-1241.

Isidori, A. (1995). *Nonlinear Control systems, 3rd Edition*, Springer, 1995.

Krstic,M., L.Kanellakopoulos & P.Kokotovic (1995). *Nonlinear and Adaptive Control Design*, John Wiley & Sons, Inc.

Joo, A. J., & J. H. Seo (1997). Design and analysis of the nonlinear feedback linearizing control for an electromagnetic suspension system, *IEEE Transactions on Control Systems Technology, 5*(1), 135-144.

Japan EM, Ltd., (1996). Manual of the magnetic levitation experimental apparatus.